ACKNOWLEDGMENTS

I thank Dr. Gale Strasburg for his valuable advice on the preparation of wheat germ calmodulin, Dr. John Gergely for critical reading of the manuscript, and also Qian Zhan for her technical assistance in this study.

REFERENCES

Babu, Y. S., Sack, J. S., Greenhough, T. J., Bugg, C. E., Means, A. R., & Cook, W. J. (1985) *Nature (London) 315*, 37-40.

Bayley, P., Martin, S., & Jones, G. (1988) *FEBS Lett. 238*, 61-66.

Cheung, W. Y. (1980) *Science (Washington, D.C.) 207*, 19-27.

Cox, J. A. (1988) *Biochem. J. 249*, 621-629.

Dale, R. E., & Eisinger, J. (1975) in *Biochemical Fluorescence: Concepts* (Chen, R. F., & Edelhoch, H., Eds.) Vol. 1, pp 115-284, Marcel Dekker, New York.

Drabikowski, W., Kuznicki, J., & Grabarek, Z. (1977) *Biochim. Biophys. Acta 485*, 124-133.

Dyson, R. D., & Isenberg, I. (1971) *Biochemistry 10*, 3233-3241.

Fairclough, R. H., & Cantor, C. R. (1978) *Methods Enzymol. 48*, 347-379.

Heidorn, D. B., & Trewhella, J. (1988) *Biochemistry 27*, 909-915.

Herzberg, O., & James, M. N. G. (1985) *Nature (London) 313*, 653-659.

Horrocks, W. DeW., Jr., & Sudnick, D. R. (1981) *Acc. Chem. Res. 14*, 384-392.

Kilhoffer, M.-C., Demaille, J. G., & Gerard, D. (1980) *FEBS Lett. 116*, 269-272.

Latt, S. A., Auld, D. S., & Vallee, B. L. (1970) *Proc. Natl. Acad. Sci. U.S.A. 67*, 1383-1389.

Manalan, S. A., & Klee, C. B. (1984) *Adv. Cyclic Nucleotide Protein Phosphorylation Res. 18*, 227-279.

Minowa, O., Yazawa, M., Sobue, K., Ito, K., & Yagi, K. (1988) *J. Biochem. (Tokyo) 103*, 531-536.

Persechini, A., Hardy, D. O., Blumenthal, D. K., Jarrett, H. W., & Kretsinger, R. H. (1988) *Biophys. J. 53*, 252a.

Small, E. W., & Anderson, S. R. (1988) *Biochemistry 27*, 419-428.

Strasburg, G. M., Hogan, M., Birmachu, W., Thomas, D. D., & Louis, C. F. (1988) *J. Biol. Chem. 263*, 542-548.

Stryer, L. (1978) *Annu. Rev. Biochem. 47*, 819-846.

Sundaralingam, M., Bergstrom, R., Strasberg, G., Rao, S. T., Roychowdhury, P., Greaser, M., & Wang, B. C. (1985) *Science (Washington, D.C.) 227*, 945-948.

Toda, H., Yazawa, M., Sakiyama, F., & Yagi, K. (1985) *J. Biochem. (Tokyo) 98*, 833-842.

Walsh, M. P., Stevens, F. C., Kuznicki, J., & Drabikowski, W. (1977) *J. Biol. Chem. 252*, 7440-7443.

Wang, C.-L. A., Tao, T., & Gergely, J. (1982a) *J. Biol. Chem. 257*, 8372-8375.

Wang, C.-L. A., Aquaron, R. R., Leavis, P. C., & Gergely, J. (1982b) *Eur. J. Biochem. 124*, 7-12.

Wang, C.-L. A., Zhan, Q., Tao, T., & Gergely, J. (1987) *J. Biol. Chem. 262*, 9636-9640.

Yoshida, M., Minowa, O., & Yagi, K. (1983) *J. Biochem. (Tokyo) 94*, 1925-1933.

Refolding of Denatured Ribonuclease Observed by Size Exclusion Chromatography†

William Shalongo, M. V. Jagannadham, Christopher Flynn, and Earle Stellwagen*

Department of Biochemistry, University of Iowa, Iowa City, Iowa 52242

Received October 31, 1988; Revised Manuscript Received February 3, 1989

ABSTRACT: The unfolding and refolding of pancreatic ribonuclease have been observed by absorbance, fluorescence, and size exclusion chromatographic measurements in solutions of guanidinium chloride continuously maintained at pH 6.0 and 4 °C. The spectral measurements were fitted with a minimal number of kinetic phases while the chromatographic measurements were simulated from an explicit mechanism. All of the measurements are consistent with a minimal mechanism involving seven components. The folded components include the native protein and two transiently stable intermediates each having the same hydrodynamic volume. The intermediate having all native peptide isomers has an unfolding midpoint in 3.8 M denaturant while the intermediate having one nonnative peptide isomer has an unfolding midpoint in 1.3 M denaturant. The unfolded protein is distributed among four components having the same hydrodynamic volume but differing peptide isomers. At equilibrium, 10% of the denatured protein has all native isomers, 60% has one nonnative isomer, 5% has a different nonnative isomer, and 25% has both nonnative isomers. In low denaturant concentrations, the dominant component with one nonnative isomer can refold to transiently populate the compact intermediate with the same nonnative isomer.

In spite of almost 2 decades of investigation, an integrated mechanism describing the unfolding/refolding reactions of ribonuclease A in denaturants has not been agreed to (Schmid, 1986; Lin & Brandts, 1987). Since all prior kinetic measurements of unfolding and refolding have utilized spectral measurements, we were optimistic that the use of an entirely different observational probe such as hydrodynamic volume measurements might make a useful contribution to definition of the mechanism. Accordingly, a series of equilibrium and kinetic measurements of the conformational transition of ribonuclease was initiated using high-performance size exclusion

†This investigation was supported by U.S. Public Health Service Research Grant GM 22109 from the Institute for General Medical Sciences.

0006-2960/89/0428-4820$01.50/0

chromatographic measurements (Shalongo et al., 1987). All laboratory manipulations were performed in 50 mM cacodylate buffer, pH 6.0 at 4 °C in the absence of ammonium sulfate and without changes in pH, in an effort to maintain a common solvent and to avoid unrecognized complications. This paper describes the analysis of such measurements and their integration with results obtained from prior spectral measurements.

Experimental Procedures

Materials. Bovine pancreatic ribonuclease A (EC 3.1.27.5), type XII-A, performic acid oxidized ribonuclease, type XII-A0, bovine pancreas trypsin inhibitor, type I-P, blue dextran, and vitamin B_{12} were purchased from Sigma. Extra pure guanidinium chloride was purchased from Heico. Toyo Soda 2000SW gel filtration columns, 7.5 × 300 mm, were purchased from Bio-Rad. These columns had an elution time for blue dextran of about 5.4 min and for solvent of about 10.3 min when operated at a flow rate of 1 mL/min.

Methods. All equilibrium and kinetic measurements of the unfolding and refolding of ribonuclease were observed in 50 mM cacodylate buffer, pH 6.0, thermostated at 4 °C unless stated otherwise. Absorbance measurements were made at 287 nm by using an Aviv Associates Model 14DS spectrophotometer, 30–78 μM ribonuclease solutions, and a 10-mm optical cell. Fluorescence measurements were made at 305 nm using 268-nm excitation, an SLM Model 4800 fluorometer, 25 μM ribonuclease solutions, and a 10-mm square optical cell. The optical cell holder of each spectrometer was thermostated by using a Neslab Endocal refrigerated circulation bath. Spectral kinetic measurements were initiated by manual mixing having a dead time of less than 15 s. Chromatographic measurements were made by using an IBM Model 9521 pump, a Rheodyne injector, an Isco Model V4 variable-wavelength detector, and an IBM Model 9000 laboratory computer. The chromatographic solvent, pump, injector, and column were all placed in a refrigerated cabinet maintained at 4 °C. Fifteen microliter samples containing 7–18 μM ribonuclease were injected into the column and subjected to isocratic chromatography at a flow rate of 1 mL/min. Equilibrium elution profiles were obtained if the denaturant concentrations in the sample and in the column were identical. Unfolding elution profiles were obtained if native protein was injected into a column containing a denaturant concentration either in the transition zone or in the denatured base-line zone. Refolding profiles were observed if protein unfolded in 7 M denaturant was injected into a column containing a denaturant concentration in the transition zone or in the native base-line zone. All elution profiles were monitored at 225 nm, a wavelength at which the absorbance of ribonuclease is independent of guanidinium concentration. The concentration of guanidinium chloride solutions was measured by using an Abbe Mark II digital refractometer. The concentration of ribonuclease was measured spectrophotometrically at 278 nm using an extinction coefficient of 9.80 mM^{-1} cm^{-1} (Sela & Anfinsen, 1957).

Kinetic spectral measurements were transmitted to a Dec Model 11/780 computer and fit with a minimum number of simultaneous first-order reactions as described previously (Kelley & Stellwagen, 1984). The individual first-order reactions in a given fit are termed kinetic phases. Each kinetic phase is characterized by a fractional amplitude and by a relaxation time. The fractional amplitude represents the change in signal amplitude associated with a given phase relative to the total change in amplitude obtained from equilibrium measurements. The relaxation time is the reciprocal of the rate constant in the direction in which the reaction is flowing. Chromatographic elution profiles were transmitted to the same computer and simulated from an explicit reaction mechanism with defined parameters as described previously (Shalongo et al., 1987). Each conformational transition was defined by a transition width, a transition midpoint, and an exchange time. The exchange time is the reciprocal sum of the forward and reverse rate constants for the reaction being considered. The exchange time and relaxation time will be coincident when either the forward or the reverse reaction dominates. The logarithm of the exchange time for a conformational transition should exhibit an inverted triangular dependence on denaturant concentration with the apex of the triangle occurring at the transition midpoint. Each configurational isomerization was defined by the percentage of the nonnative isomer at equilibrium and by an exchange time for isomerization. In contrast to the conformational transition, the exchange time for a configurational isomerization is independent of denaturant concentration for a given protein conformation. The parameters for the conformational transitions and for the configurational isomerizations in a given mechanism were varied until the simulated and observed elution profiles could be globally fit with a constant transition width and midpoint for each conformational transition and a constant percentage nonnative isomer and exchange time for each configurational isomerization.

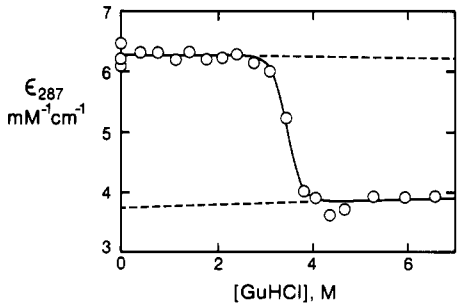

FIGURE 1: Absorbance spectral measurements. The absorbance of a 30 μM solution of ribonuclease in 50 mM cacodylate buffer, pH 6.0, was measured as a function of guanidinium chloride (GuHCl in figures) concentration at 4 °C. The dashed lines represent least-squares analysis of the experimental values in the native and denatured base-line zones. The solid line represents the transition predicted by the mechanism in Figure 6 and the exchange times in Figure 4 assuming that all the compact forms have the extinction coefficient described by the extrapolated native base-line relationship and that all the denatured forms have the extinction coefficient described by the extrapolated denatured base-line relationship.

Results

Equilibrium Measurements. The reversible equilibrium denaturation transition for ribonuclease observed in guanidinium chloride at 4 °C using absorbance measurements at 287 nm is shown in Figure 1. The midpoint of the equilibrium transition is at 3.45 M which is within the range observed for mammalian ribonucleases at 10 °C, 3.35 ± 0.10 M (Kreb et al., 1985). The central 80% of the transition, defined here as the transition width, occurred within 0.8 M denaturant. All conformation transitions in the chromatographic simulations were assumed to have this width. The equilibrium transition shown in Figure 1 serves to define three denaturant concentration zones: less than 3 M is the native base-line zone, 3–4 M inclusive is the transition zone, and greater than 4 M is the denatured base-line zone.

Representative chromatographic elution profiles observed at equilibrium in the native base-line zone, in the transition zone, and in the denatured base-line zone are illustrated in Figure 2. The dependence of the elution time of ribonuclease on denaturant concentration is illustrated in Figure 3. This dependency is compared with that of a persistent denatured

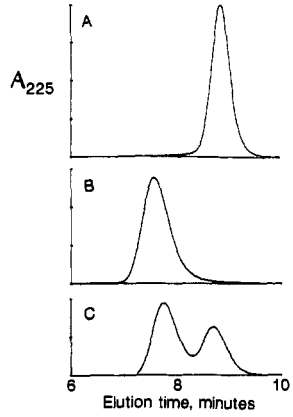

FIGURE 2: Equilibrium elution profiles for ribonuclease. All profiles were observed at 4 °C using solvents containing 50 μM cacodylate buffer, pH 6.0, and the following concentrations of GuHCl: panel A, 2.0 M; panel B, 5.5 M; panel C, 3.6 M. The ordinate is the absorbance at 225 nm expressed in millivolts and is scaled identically in each panel. The profile simulated by the mechanism in Figure 6 and the parameters shown in Figure 4 superimposes that observed in panel C.

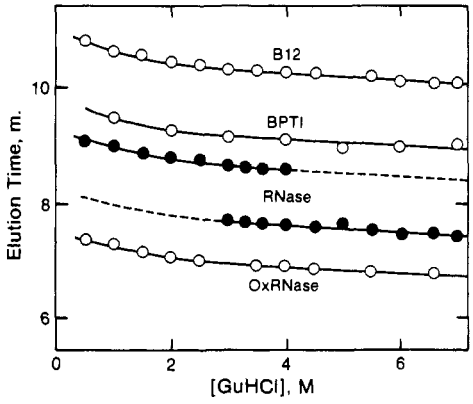

FIGURE 3: Dependence of elution time on denaturant concentration. Both the samples and the isocratic chromatographic solvent contained 50 mM cacodylate buffer, pH 6, and the indicated concentrations of guanidinium chloride and were maintained at 4 °C. The observed elution times for vitamin B_{12} (B12), bovine pancreatic trypsin inhibitor (BPTI), and performic acid oxidized ribonuclease (OxRNase) are indicated by open circles and are each connected by a single line. The observed elution times for unmodified ribonuclease (RNase) are indicated by closed circles and are connected by two lines representing the native (upper) and denatured (lower) protein. The elution time for blue dextran was 5.44 ± 0.02 min, and the elution time for water, observed as a refractive discontinuity, was 10.32 ± 0.04 min in all these solvents.

protein, performic acid oxidized ribonuclease, with a persistent globular protein, pancreatic trypsin inhibitor, and with an included small molecule, vitamin B_{12}. Each of these molecules exhibits a common curvilinear dependence on denaturant concentration, suggesting that each of them can bind with the matrix during chromatography and that such binding diminishes with increasing denaturant concentration. The equilibrium elution profile for ribonuclease in each base-line zone is nearly symmetrical, as shown in Figure 2, and similar in shape to that observed for pancreatic trypsin inhibitor and for oxidized ribonuclease. Model calculations of matrix binding indicate (i) that such near-symmetry results from on and off rates for binding having half-times less than 1 s, (ii) that the curvilinear dependence of elution time on denaturant concentration requires that well under 10% of the protein in a column is bound to the matrix at any one time, and (iii) that this matrix binding only modestly perturbs analysis of protein conformational transitions by size exclusion chromatographic measurements. A detailed discussion of matrix binding and its effect on conformational analysis will be considered in a separate paper.

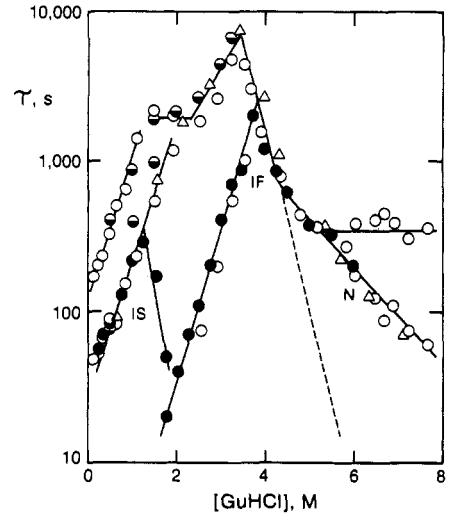

FIGURE 4: Dependence of kinetic parameters on denaturant concentration. The open triangles indicate relaxation times obtained from absorbance measurements. The open circles indicate relaxation times obtained from fluorescence measurements. The half-filled circles indicate relaxation times for fluorescence measurements simulated from the mechanism shown in Figure 6 and assuming the following relative fluorescence amplitudes (Rehage & Schmid, 1982): N = IF = 0.0; IS = 0.3; UF = UF′ = 0.7; US = US′ = 1.0. The closed circles indicate exchange times obtained from simulation of chromatographic elution profiles. The inverted triangles for the conformational transitions of IS and of IF are labeled at their apexes while the fragment of the triangle for N is labeled just below its unfolding arm.

Equilibrium chromatographic elution profiles observed in the transition zone are all bimodal with a well-defined valley as illustrated by the elution profile obtained in 3.6 M denaturant in Figure 2C. Such bimodal profiles are characteristic for a conformational transition having a slow exchange time. Indeed, simulation of this profile as a two-state transition would require a midpoint of 3.41 M and an exchange time of 4000 s. Such a slow exchange time predicts that the elution times for the denatured and native components in the transition zone would be continuous with the relationships observed in the base-line zones. This is the case as shown in Figure 3. We find that the chromatographic profiles observed in all zones can be simulated by assuming that the elution times for the folded and unfolded forms of ribonuclease differ by 1.05 ± 0.05 min. This difference is compatible with the results shown in Figure 3.

Unfolding Measurements. The change in tyrosine absorbance accompanying the unfolding of ribonuclease in the transition zone and in the denatured base-line zone can each be fit with a single kinetic phase at 4 °C as is the case at 10 °C (Krebs et al., 1985). In each unfolding measurement, the single phase accounts for all the change in absorbance anticipated from the equilibrium measurements shown in Figure 1. The denaturant concentration dependence of relaxation time for the single unfolding phase observed by absorbance measurements at 4 °C is denoted by the open triangles in Figure 4. The relaxation time for unfolding in 4.7 M at 4 °C is within the range of values predicted from measurements in the same solvent at 10 °C, 150 ± 30 s, using an activation energy of 25 ± 1 kcal/mol (Krebs et al., 1985).

All the anticipated change in tyrosine fluorescence amplitude accompanying unfolding at 4 °C in the transition zone and in a portion of the denatured base-line zone also fits well with a single phase. However, for denaturant concentrations greater than 6 M, two phases are required to fit the observed changes

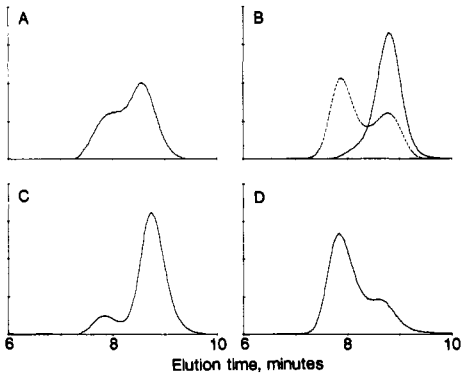

FIGURE 5: Kinetic elution profiles. Panel A illustrates the unfolding profile observed in 4.5 M denaturant following injection of native protein. This profile can be simulated equally well by N–UF having a midpoint of 3.8 M and an exchange time of 625 s, by N–IF–UF in which N–IF has a midpoint of 3.8 M and an exchange time of 625 s and IF–UF has a midpoint of 3.8 M and an exchange time of 400 s, or by the mechanism shown in Figure 6 using the exchange times indicated in Figure 4. Such multiplicity results because the rate-limiting step either involves the change in hydrodynamic volume, N–UF, or precedes this step, N–IF–UF, and because the reactions in the denatured state do not involve a detectable change in hydrodynamic volume. Panel B illustrates the refolding profile observed in 0.35 M denaturant following injection of unfolded protein equilibrated in 7.0 M denaturant. The dashed profile would be observed if component IS were not populated in the mechanisms shown in Figure 6. Panel C illustrates the refolding profile observed in 2.5 M denaturant following injection of protein unfolded for 120 s in 7.0 M denaturant. The information in Figures 4 and 6 predicts that the sample injected would contain 34% N, 51% UF, 10% US, 3% UF′, and less than 1% IF and US′. The profile was simulated by using the mechanism in Figure 6 and the exchange times in Figure 4. Panel D illustrates the refolding profile observed in 2.5 M denaturant following injection of unfolded protein equilibrated for 43 200 s in 7.0 M denaturant. The ordinate in each panel represents the absorbance at 225 nm expressed in millivolts.

in fluorescence amplitude at 4 and at 10 °C (Krebs et al., 1985). The denaturant concentration dependence of the relaxation times for both unfolding phases observed by fluorescence measurements at 4 °C is denoted by the open circles in Figure 4. It should be noted that the denaturant-dependent unfolding relaxation times obtained from both absorbance and fluorescence measurements are in common at 4 °C (Figure 4) and at 10 °C (Krebs et al., 1985). The relaxation time unique to the fluorescence measurements is independent of denaturant concentration and accounts for 0.31 ± 0.03 of the equilibrium amplitude at 4 and 10 °C (Rehage & Schmid, 1982). The relaxatin time of the guanidine-independent reaction at 4 °C, 350 ± 40 s, is compatible with the relaxation time of the guanidine-independent reaction at 10 °C, 163 ± 16 s, using the activation energy of 22.0 kcal/mol (Rehage & Schmid, 1982). Schmid et al. (1986) have assigned this guanidine-independent reaction to the cis/trans isomerization of peptide bond Tyr^{92}–Pro^{93}.

Chromatographic unfolding profiles in the transition zone and in the native base-line zone are characteristic for continuous unfolding of native protein during chromatography as illustrated in Figure 5A. Each of the unfolding profiles could be simulated by using a two-state mechanism having a midpoint at 3.8 M denaturant. The denaturation concentration dependence of the exchange times for unfolding at 4 °C obtained from chromatographic simulations is denoted by the closed circles in Figure 4. It should be noted that the exchange times are in common with the relaxation times for the denaturant-dependent unfolding reaction observed by using either absorbance measurements (open triangles) or fluorescence measurements (open circles). However, the abrupt change in slope at 4.3 M denaturant indicates that more than one denaturant-dependent kinetic event is being observed spectrally and chromatographically during unfolding. This change in slope has not been observed previously because unfolding has been systematically measured only below 4.4 M denaturant (Lang et al., 1986) and not linked with single measurements in 4.7 M denaturant (Krebs et al., 1985) and in 5.0 and 7.0 M denaturant (Rehage & Schmid, 1982).

A minimal solution to observation of an abrupt change in slope described by a single kinetic phase suggests two coupled reactions in which the rate-limiting step changes from one reaction to the other. All the unfolding chromatographic profiles can be simulated by using the mechanism N–IF–UF assuming (i) that N and IF have the same hydrodynamic volume, (ii) that the reaction IF–UF has a midpoint at 3.8 M and is rate limiting in denaturant concentrations below 4.3 M, and (iii) that the reaction N–IF has a midpoint near 3.8 M and is rate limiting in more concentrated denaturant solutions. The exchange times simulated for the reaction IF–UF are indicated by the solid and dashed lines forming the descending limb of the inverted triangle labeled IF in Figure 4. The exchange times simulated for the reaction N–IF are indicated by the solid line labeled N in Figure 4.

Refolding Measurements. Refolding fluorescence measurements initiated by using protein equilibrated with 7 M denaturant could be fit with two kinetic phases throughout the transition zone and the native base-line zone. However, the relative amplitudes of these two phases and their relaxation time relationships varied widely within the native base-line zone, indicating the occurrence of alternative folding pathways. The fluorescence refolding relaxation times are denoted by the open circles below 3.5 M denaturant in Figure 4. For refolding measurements obtained in denaturant concentrations greater than 2.5 M, 5 ± 1% of the amplitude change occurred in a fast phase and the remaining amplitude in a slow phase. Below 2.5 M denaturant, the relaxation time for fast-phase refolding exceeds the capacity for measurement by manual mixing although the amplitude for the fast phase persists as missing amplitude. Below 2.5 M denaturant, the relaxation time for slow-phase refolding assumes a denaturant-independent value of 1985 ± 215 s. Amplitude progressively disappears from this slow phase and reappears in one and then two new phases whose relaxation times are indicated in Figure 4 below 2 M denaturant. The ratio of the relaxation times for these two new folding phases in 0.5 M denaturant is 4.9 at 4 °C compared with 6.0 at 10 °C (Schmid, 1983). The fractional amplitude of the more rapid of these two new refolding phases gradually increases until it reaches a limiting value of 0.75 ± 0.03 in denaturant concentrations below 0.5 M at 4 °C. This compares favorably with a limiting value of 0.81 ± 0.07 at 10 °C (Schmid, 1983).

Refolding absorbance measurements initiated with the same denatured protein proceed through a similar scenario with respect to changes in amplitude and phase designation. The relaxation times obtained from refolding absorbance measurements at 4 °C are denoted by open triangles below 3.5 M denaturant in Figure 4. It should be noted that the relaxation times obtained from refolding absorbance measurements agree quite well with those obtained from refolding fluorescence measurements.

Refolding chromatographic profiles observed throughout the transition zone and the native base-line zone were dependent upon the exposure time of native protein to excess denaturant prior to injection in the column to initiate refolding. For example, the refolding profiles observed in 2.5 M denaturant

upon injection of protein exposed to 7.0 M denaturant for 120 s and for 43 200 s are distinct as illustrated in Figure 5, panels C and D, respectively. This distinction does not result from continued unfolding with time, which can be predicted from the exchange time in Figure 4, but from conversion of a fast-folding to a slow-folding form in 7.0 M denaturant prior to initiation of refolding. This conversion can be incorporated into the emerging mechanism for the refolding of ribonuclease as a coupled reaction linking UF with US. Refolding profiles initiated from protein unfolded for 120 s in 7.0 M denaturant were simulated by using the mechanism N–IF–UF–US assuming (i) the same hydrodynamic volume for UF and US, (ii) an exchange time of 300 s for UF–US, (iii) 75% of the unfolded protein is US at equilibrium, and (iv) a midpoint of 3.8 M for IF–UF. These assumptions facilitate estimation of the exchange times for the reaction IF–UF during refolding. The resultant exchange times are denoted by the closed circles which form the ascending limb of the inverted triangle labeled IF in Figure 4.

Refolding profiles initiated with unfolded protein equilibrated with 7.0 M denaturant are identical with that illustrated in Figure 5D over the denaturant concentration range 2.0–3.0 M. This identity indicates that the slow obligatory US–UF conversion precedes folding in this denaturant concentration range. However, refolding profiles observed in denaturant concentrations below 2.0 M increasingly evidence much more refolding as illustrated in Figure 5, panel B. This would result if an alternative refolding pathway became operative at low concentrations in which the slow event in the denatured state was no longer obligatory. One such pathway involves the transient compact intermediate IS which directly links components IF and US in the mechanism N–IF–UF–US. Simulations of refolding profiles observed below 2.0 M denaturant initiated by using unfolded protein equilibrated in 7.0 M denaturant facilitate estimation of the midpoint and exchange time for the reaction IS–US assuming (i) the five-component mechanism, (ii) N, IF, and IS each have the same hydrodynamic volume, and (iii) the midpoints, exchange times, and equilibrium concentrations estimated above. Unfortunately, the five-component mechanism does not generate a consistent midpoint and inverted triangle for the IS–US reaction owing to the abundance of unfolded protein in refolding profiles observed below 1.0 M denaturant. However, all the refolding profiles could be simulated by using a common midpoint of 1.3 M and the inverted triangle labeled IS in Figure 4 by assuming a second slow isomerization event in the unfolded protein. Such simulations require that the second isomerization is 40% in a nonnative unfolded isomer at equilibrium and has an exchange time with its native unfolded isomer of 300 s.

The second isomerization extends the five-component mechanism to the seven-component mechanism illustrated in Figure 6. The occurrence of two isomerization events in the unfolded protein generates two components, US and UF′, each having one nonnative isomer and one component, US′, having two nonnative isomers. The percentile distribution of protein among the four unfolded forms is listed in Figure 6 as well as the midpoint values for two of the folding reactions, IF–UF and IS–US. This complete mechanism combined with the exchange times denoted by the closed circles in Figure 4 will simulate all the observed refolding chromatographic profiles initiated by using protein unfolded in 7.0 M denaturant either for 120 s or for 43 200 s.

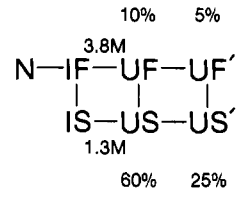

FIGURE 6: Mechanism for the folding of ribonuclease. Component N is native ribonuclease; IF and IS are compact intermediate forms having the same hydrodynamic volume as N; and UF, US, UF′, and US′ are unfolded forms each having the same hydrodynamic volume as denatured ribonuclease. Components N, IF, and UF each have all-native peptide bond isomers. IS and US each have one and the same nonnative peptide bond isomer. UF′ has a different nonnative peptide isomer bond, and US′ has both nonnative peptide bond isomers. At equilibrium, [IF]/[IS] = 1000, [UF]/[US] = [UF′]/[US′] = 0.18, and [UF]/[UF′] = [US]/[US′] = 2.33. The distribution of unfolded protein among the four denatured components at equilibrium is indicated by the percentage values on the figure. The midpoint values for the conformational transitions UF–US and IS–US are indicated in the figure in molar units of denaturant concentration. The exchange time among the denatured forms is 300 s and is denaturant independent. The exchange time for IF–IS can range from 100 to 200 s and simulate the chromatographic patterns equally well.

Discussion

The simulation of the chromatographic elution profiles was begun from a simple two-state mechanism, and additional reactions were coupled on as required. All of the unfolding and refolding chromatographic profiles obtained can be fit with the mechanism illustrated in Figure 6 using the exchange times illustrated by the closed circles in Figure 4. Elements of this mechanism have been previously considered by several investigative groups. The generation of two (Cook et al., 1979; Schmid & Blaschek, 1981) or three (Lin & Brandts, 1983) slow-folding forms in the denatured state has been recognized for some time. Schmid et al. (1986) assign the UF–US reaction in Figure 6 to the cis/trans isomerization of peptide bond Tyr^{92}–Pro^{93} based on fluorescence measurements while Lin and Brandts (1983) assign the same peptide isomerization to the UF–UF′ reaction in Figure 6 based on isomer-specific proteolysis measurements. Irrespective of assignment, both Schmid (1983) and Lin and Brands (1987) consider that US can refold into a compact conformation in low denaturant concentrations, a reaction denoted as IS–US in the mechanism of Figure 6. It should be noted that the refolding profiles also require the folding of the major denatured component, US, prior to peptide isomerization, as illustrated in Figure 5, panel B. The compact product of this folding, IS, contains a single nonactive peptide bond and is likely equivalent to component IN described by Schmid (1983, 1986). By contrast, the refolding profiles do not require direct refolding of the denatured components UF′ and US′ prior to isomerization of the primed components. This may reflect the low abundance of UF′ and a midpoint less than 0.3 M denaturant for a compact intermediate having two nonnative peptide isomers, IS′.

The mechanism shown in Figure 6 characterizes the transition midpoints of the individual folding reactions previously considered. The midpoint for the fast-folding reaction, IF–UF, was fit with a value of 3.8 M. The coupling of this folding reaction with the four isomerization reactions in the denatured state lowers the midpoint of the overall reaction in the denatured state to 3.45 M as illustrated in Figure 1. The midpoint for the slow-folding reaction, IS–US, was fit with a value of 1.3 M. The difference in the midpoint values of IF and IS suggests that the presence of a nonnative peptide isomer diminishes the stability of the compact structure of ribonuclease by about 8 kcal/mol.

The mechanism shown in Figure 6 adds one new component to the mechanisms previously considered. A compact folding intermediate IF has been introduced to accommodate the abrupt change in slope in the denaturant dependence of the

relaxation/exchange times for unfolding. Chromatographic simulations require that the unfolding reaction IF–UF is rate limiting in denaturant concentration below 4.5 M and that the unfolding reaction N–IF is rate limiting in more concentrated denaturant solutions. Since the reaction N–IF occurs subsequent to the change in hydrodynamic volume accompanying refolding, we cannot use chromatographic measurements to establish the midpoint for the reaction N–IF. However, unfolding profiles require that its midpoint be near 3.8 M while symmetry considerations for the inverted triangular relationship would suggest that its relaxation time ranges from about 100 to 600 s in the native base-line zone.

The mechanism and exchange times in Figures 4 and 6 predict several equilibrium and kinetic features of ribonuclease which were not involved in the development of the mechanism. First, both the equilibrium transition curve and the equilibrium chromatographic profiles obtained in the transition zone are predicted, as illustrated in Figures 1 and 2C. Second, the exchange times for the refolding kinetic phases observed by fluorescence measurements are predicted, as illustrated by the half-filled circles at 0.5 M denaturant intervals in Figure 4. It should be noted that the relaxation times predicted and observed for spectral measurements often extend to slower times than obtained by simulation of chromatographic profiles. This is because spectral measurements observe the net relaxation time of coupled reactions while the chromatographic simulations consider the parameters of the individual reactions which are coupled. In addition, the spectral measurements are fit with unidirectional or one-way relaxation times whereas the exchange times obtained from chromatographic simulations are bidirectional or two-way values. Accordingly, the spectral measurements observe and the mechanism predicts the elevated inverted triangle having an apex at 3.4 M. This triangle results from the juncture of the denaturant dependence of the relaxation times for two different reactions, namely, fast unfolding and a slow refolding requiring peptide isomerization prior to refolding. This same triangle has been previously observed (Lang et al., 1986) for a variety of mammalian ribonucleases. It should be noted that the slow-folding phase reaches the limiting relaxation time of 1985 ± 215 s predicted by the mechanism and observed as the flat line between 1.5 and 2.5 M denaturant in Figure 4. This slow-refolding phase gradually disappears as folding intermediates containing nonnative peptide isomers become transiently populated. Third, the mechanism predicts the fast-folding phase originating from UF. Extrapolation of the refolding arm of the triangle labeled IF predicts the refolding times in the millisecond time range observed in low denaturant concentrations (Garel et al., 1976; Hagerman & Baldwin, 1976).

Registry No. Ribonuclease, 9001-99-4.

References

Cook, K. H., Schmid, F. X., & Baldwin, R. L. (1979) *Proc. Natl. Acad. Sci. U.S.A. 76*, 6157–6161.

Garel, J.-R., Nall, B. T., & Baldwin, R. L. (1976) *Proc. Natl. Acad. Sci. U.S.A. 73*, 1853–1857.

Hagerman, P. J., & Baldwin, R. L. (1976) *Biochemistry 15*, 1462–1473.

Kelley, R. F., & Stellwagen, E. (1984) *Biochemistry 23*, 5095–5102.

Krebs, H., Schmid, F. X., & Jaenicke, R. (1985) *Biochemistry 24*, 3846–3852.

Lang, K., Wrba, A., Krebs, H., Schmid, F. X., & Beintema, J. J. (1986) *FEBS Lett. 204*, 135–139.

Lin, L.-N., & Brandts, J. F. (1983) *Biochemistry 22*, 573–580.

Lin, L.-N., & Brandts, J. F. (1987) *Biochemistry 26*, 1826–1830.

Rehage, A., & Schmid, F. X. (1982) *Biochemistry 21*, 1499–1505.

Schmid, F. X. (1981) *Eur. J. Biochem. 114*, 105–109.

Schmid, F. X. (1983) *Biochemistry 22*, 4690–4696.

Schmid, F. X. (1986) *FEBS Lett. 198*, 217–220.

Schmid, F. X., & Blaschek, H. (1981) *Eur. J. Biochem. 114*, 111–117.

Schmid, F. X., Grafl, R., Wrba, A., & Beintema, J. J. (1986) *Proc. Natl. Acad. Sci. U.S.A. 83*, 872–876.

Sela, M., & Anfinsen, C. B. (1957) *Biochim. Biophys. Acta 24*, 229–235.

Shalongo, W., Ledger, R., Jagannadham, M. V., & Stellwagen, E. (1987) *Biochemistry 26*, 3135–3141.